

## Supplementary Information

# Constructing CuNi Dual Active Sites on ZnIn<sub>2</sub>S<sub>4</sub> for Highly Photocatalytic Hydrogen Evolution

Jingyi Jin<sup>†</sup>, Yanren Cao<sup>†</sup>, Ting Feng<sup>†</sup>, Yanxin Li<sup>†</sup>, Ruonan Wang<sup>†</sup>, Kaili Zhao<sup>†</sup>, Wei Wang<sup>†,§</sup>, Bohua Dong<sup>†,\*</sup>, Lixin Cao<sup>†,\*</sup>

<sup>†</sup> School of Materials Science and Engineering, Ocean University of China, Qingdao 266100, China

<sup>§</sup> Aramco Research Center-Boston, Aramco Services Company, Cambridge, MA 02139, USA

\* Corresponding author. Tel.: +86 13864808725; fax: +86 0532 66781901

E-mail address: [caolixin@ouc.edu.cn](mailto:caolixin@ouc.edu.cn) (Lixin Cao); [dongbohua@ouc.edu.cn](mailto:dongbohua@ouc.edu.cn) (Bohua Dong)

## EXPERIMENTAL SECTION

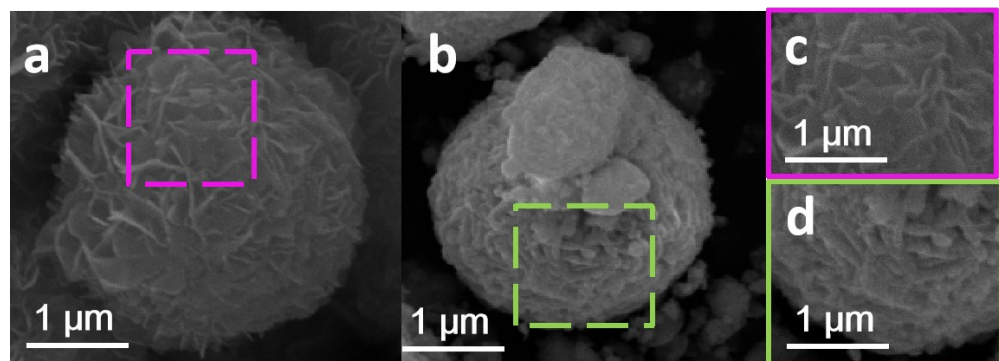


Fig. S1 SEM images of (a) pure ZnIn<sub>2</sub>S<sub>4</sub> and (b) 12% Cu<sub>2</sub>Ni<sub>1</sub>-ZIS. The enlarged images of (c) pure ZnIn<sub>2</sub>S<sub>4</sub> and (d) 12% Cu<sub>2</sub>Ni<sub>1</sub>-ZIS.

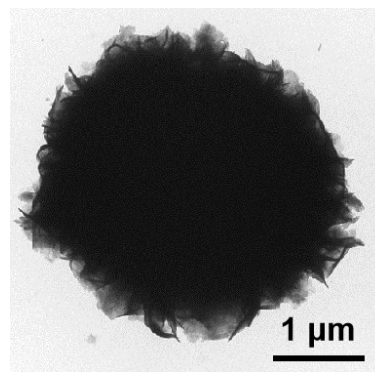


Fig. S2 TEM image of pure ZnIn<sub>2</sub>S<sub>4</sub>.

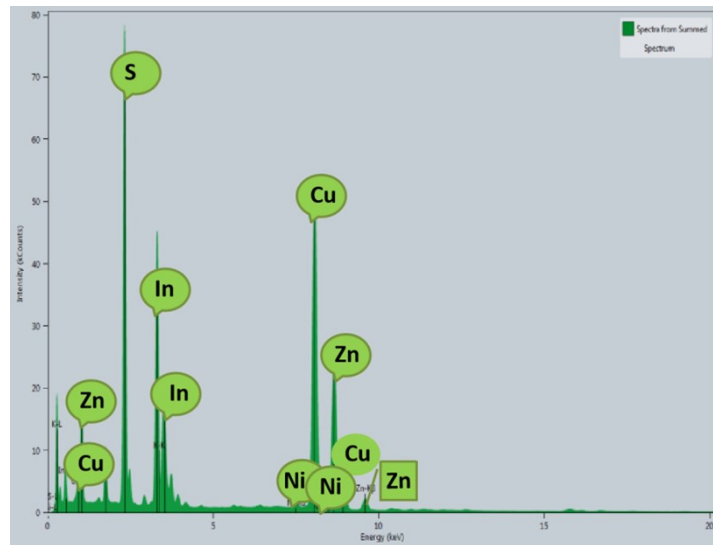


Fig. S3. The EDS spectrum of 12% Cu<sub>2</sub>Ni<sub>1</sub>-ZIS

Table S1. The surface element content from XPS characterization.

Element	Atomic %	Element	Atomic %
S	31.05	Cu	0.85
Zn	17.68	Ni	0.55
In	10.56	C	28.89
N	2.95	O	7.47
<b>Exact mass ratio of Cu to ZnIn<sub>2</sub>S<sub>4</sub> = 1.62%</b>		<b>Exact mass ratio of Ni to ZnIn<sub>2</sub>S<sub>4</sub>= 0.97%</b>	

Table S2 Performance comparison of ZnIn<sub>2</sub>S<sub>4</sub> modified by different types of cocatalyst

Category	Cocatalyst	Illumination conditions	Sacrifice agent	H <sub>2</sub> evolution Rate (μmol g <sup>-1</sup> ·h <sup>-1</sup> )	α*	Ref.
Bi-metals	<b>Cu-Ni</b>	<b>λ≥420 nm</b>	<b>0.35 M Na<sub>2</sub>S 0.25 M Na<sub>2</sub>SO<sub>3</sub></b>	<b>7825</b>	<b>29.5</b>	<b>This work</b>
	Co-Ni	λ>420 nm	Ascorbic acid	3336.6	4.3	[1]
	Co-P	λ>420 nm	Lactic acid	7840	44.0	[2]
Noble metal	Au	λ>420 nm	None	1633.4	4.41	[3]
	Pt	λ>420 nm	140 mmol Na <sub>2</sub> S 100 mmol Na <sub>2</sub> SO <sub>3</sub>	1150	7.57	[4]
Metal oxides	Ag <sub>2</sub> O	full spectrum	Triethanolamine	2334.19	3.39	[5]
	WO <sub>3</sub>	λ>420 nm	0.25 M Na <sub>2</sub> SO <sub>3</sub> 0.35 M Na <sub>2</sub> S	2202.9	5.22	[6]
Metal sulfides	MoS <sub>2</sub>	λ>420 nm	Lactic acid	2512.5	8.73	[7]
		λ≥420 nm	0.43 M Na <sub>2</sub> S 0.5 M Na <sub>2</sub> SO <sub>3</sub>	2060	10.85	[8]
	MoSe <sub>2</sub>	λ>420 nm	Na <sub>2</sub> S, Na <sub>2</sub> SO <sub>3</sub>	2228	2.18	[9]
Others	Ni <sub>2</sub> P	λ≥400 nm	Lactic acid	2066	4.43	[10]
	CQD-Pt	λ>420 nm	Triethanolamine	1032.2	11.21	[11]
	rGO-Pt	λ>420 nm	0.25 M Na <sub>2</sub> SO <sub>3</sub> 0.35 M Na <sub>2</sub> S	1210	26.3	[12]

\* A parameter of α is adopted to describe the cocatalytic performance, which is defined by the quotient of the reaction rate of ZIS with cocatalysts and that of pure ZnIn<sub>2</sub>S<sub>4</sub> without cocatalysts in each paper.

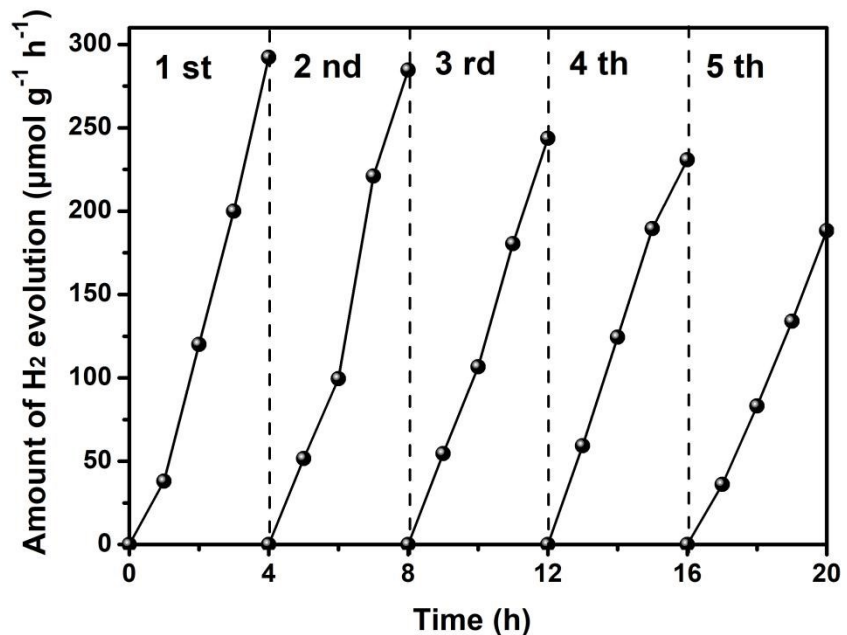


Figure S4. Stability test of pure  $\text{ZnIn}_2\text{S}_4$  under the same condition as mentioned in this paper

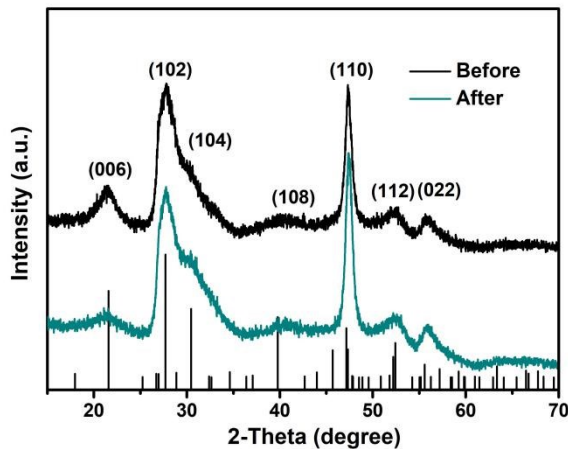


Figure S5. The XRD spectrum of 12%  $\text{Cu}_2\text{Ni}_1\text{-ZIS}$  before and after stability test

The XRD spectrum of 12%  $\text{Cu}_2\text{Ni}_1\text{-ZIS}$  after 20 h stability test didn't display evident characteristic peak migration compared with previous 12% $\text{Cu}_2\text{Ni}_1\text{-ZIS}$  except the peak intensity of (006) lattice plane decreased a little.

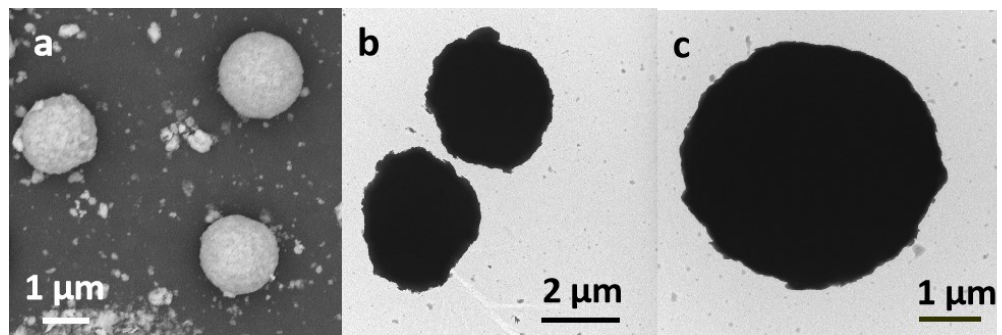


Fig. S6 (a) SEM (b-c) TEM images of 12% Cu<sub>2</sub>Ni<sub>1</sub>-ZIS after stability test.

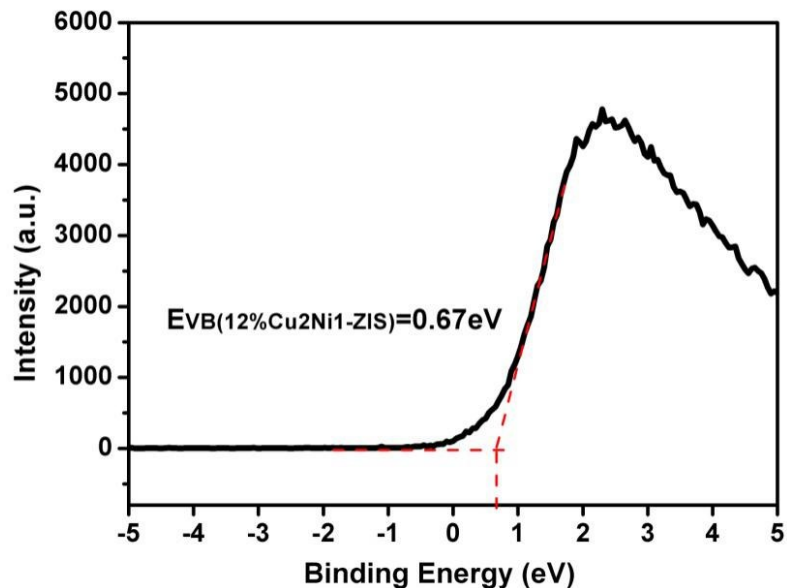


Figure S7 XPS valence band spectrum for 12%Cu<sub>2</sub>Ni<sub>1</sub>-ZIS showing the edge of valence band

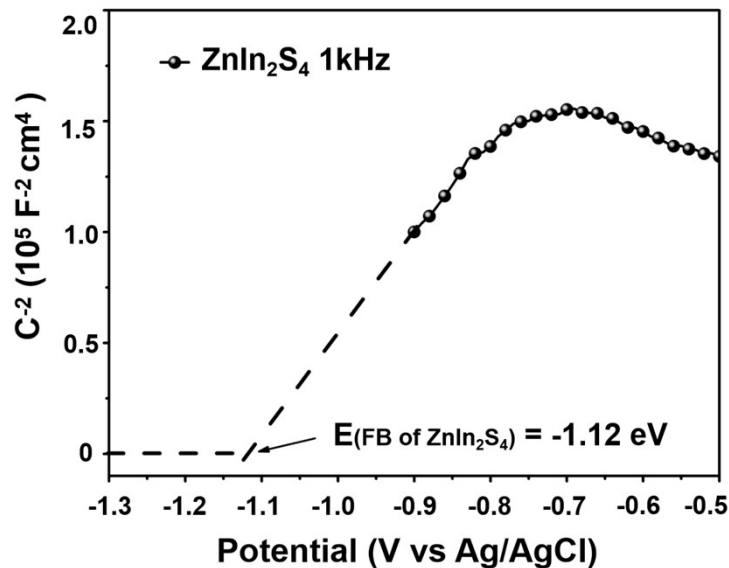


Figure S8 Mott-Schottky curve of pure  $\text{ZnIn}_2\text{S}_4$

Mott-Schottky curves were taken at 1.0 kHz frequency. The potential ranged from -1.3 V to -0.5 V (vs. Ag/AgCl), and the modulation amplitude of 5 mV. The 0.5 M  $\text{Na}_2\text{SO}_4$  was used as the electrolyte solution.

According to Fig. S8, the flat band (FB) potential is -1.12 V (vs. Ag/AgCl). In general, the flat band potential of n-type semiconductors obtained from Mott-Schottky curves is about 0.2 V more positive than its conduction band potential [13]. Therefore, the conduction band potential of  $\text{ZnIn}_2\text{S}_4$  is about -1.32 V vs. Ag/AgCl. According to the following equation:

$$E_{FB}(\text{vs. NHE}) = E_{FB}(\text{vs. Ag/AgCl}) + 0.197$$

The conduction band of  $\text{ZnIn}_2\text{S}_4$  is -1.13 V vs. NHE. Combining its band gap (2.54 eV), the valence band potential of  $\text{ZnIn}_2\text{S}_4$  is 1.41 V vs. NHE.

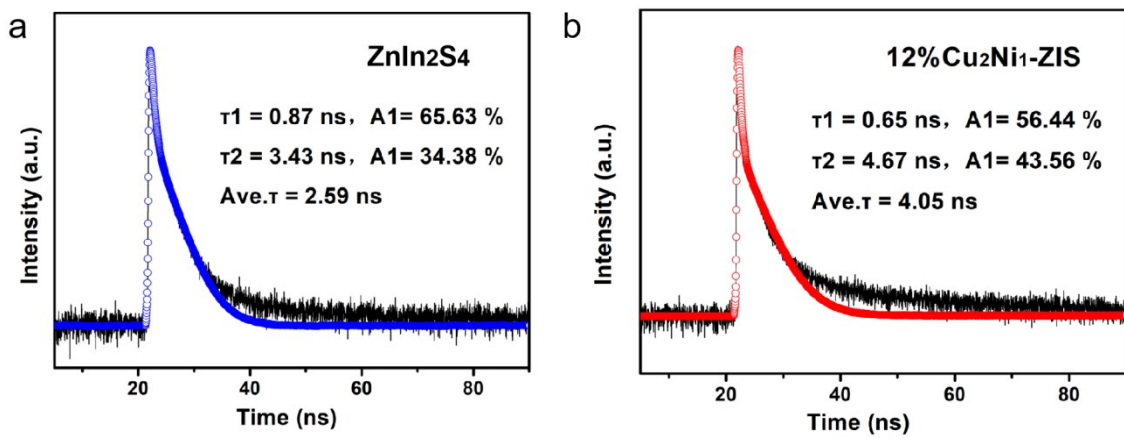


Figure S9 Transient-state photoluminescence spectra: (a) ZnIn<sub>2</sub>S<sub>4</sub> (b) 12% Cu<sub>2</sub>Ni<sub>1</sub>-ZIS

Table S3 Fluorescence emission lifetime and relevant percentage data of ZnIn<sub>2</sub>S<sub>4</sub> and 12%Cu<sub>2</sub>Ni<sub>1</sub>-ZIS

Samples	$\tau_1$ (ns)	A <sub>1</sub> (%)	$\tau_2$ (ns)	A <sub>2</sub> (%)	Average lifetime ( $\tau_a$ ) (ns)
ZnIn <sub>2</sub> S <sub>4</sub>	0.87	65.62	3.43	34.38	2.59
12%Cu <sub>2</sub> Ni <sub>1</sub> -ZIS	0.65	56.44	4.67	43.56	4.05

The fitted parameters of the above transient-state photoluminescence spectra are acquired via the following bi-exponential formulas:

$$I(t) = I_0 + A_1 \exp(-t/\tau_1) + A_2 \exp(-t/\tau_2)$$

The above average lifetime value is obtained according to the following formulas:

$$\tau_a = (A_1\tau_1^2 + A_2\tau_2^2)/(A_1\tau_1 + A_2\tau_2)$$

where  $I_0$  is the baseline correction value,  $A_1$  and  $A_2$  represent the bi-exponential factors.  $A_1$ ,  $A_2$  represent the double exponential factors.  $\tau_1$ ,  $\tau_2$  and  $\tau_a$  corresponding the lifetime in different stages (radiation, non-radiation) and average lifetime respectively.

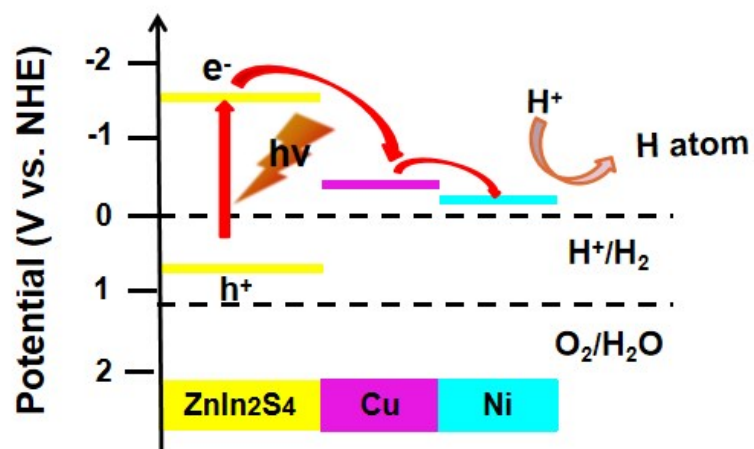


Figure S10 The energy level position and mechanism of electrons migration in 12%Cu<sub>2</sub>Ni<sub>1</sub>-ZIS

## Reference

- (1) Z.-J. Li, X.-H. Wang, W.-L. Tian, A. Meng and L.-N. Yang, *ACS Sustain. Chem. Eng.*, 2019, **7**, 20190-20201.
- (2) Q.-W. Liu, M.-D. Wang, Y.-S. He, X.-X. Wang and W.-Y. Su, *Nanoscale*, 2018, **10**,

19100-19106.

- (3) T.-T.Zhu, X.-J.Ye, Q.-Q. Zhang, Z.-Z. Hui, X.-C. Wang and S.-F. Chen, *J. Hazard Mater.*, 2019, **367**, 277-285.
- (4) L. Shang, C. Zhou, T. Bian, H.-J. Yu, L.-Z. Wu, C.-H. Tung and T.-R.Zhang, *J. Mater. Chem. A*, 2013, **1**, 4552-4558.
- (5) Y. Xiao, Z.-Y. Peng, W.-L.Zhang, Y.-H. Jiang and L. Ni, *Appl. Surf. Sci.* 2019, **494**, 519-531.
- (6) P.-F. Tan, A.-Q.Zhu, L.-L. Qiao, W.-X. Zeng, Y.-J. Ma, H.-G. Dong, J.-P. Xie and J. Pan, *Inorg. Chem. Front.*, 2019, **6**, 929-939.
- (7) C. Liu, B. Chai, C.-L. Wang, J.-T. Yan and Z.-D. Ren, *Int. J. Hydrogen Energy*, 2018, **43**, 6977-6986.
- (8) L. Wei, Y.-J. Chen, Y.-P. Lin, H.-S. Wu, R.-S. Yuan and Z.-H. Li, *Appl. Catal. B Environ.* 2014, **144**, 521-527.
- (9) D.-Q.Zeng, L. Xiao, W.-J. Ong, P.-Y. Wu, H.-F. Zheng, Y.-Z. Chen and D.-L.Peng, *Chemsuschem* 2017, **10**, 4624-4631.
- (10) X.-L. Li, X.-J.Wang, J.-Y. Zhu, Y.-P. Li, J. Zhao and F.-T. Li, *Chem. Eng. J.*, 2018, **353**, 15-24.
- (11) Q. Li, C. Cui, H. Meng and J.-G. Yu, *Chem. Asian J.*, 2014, **9**, 1766-1770.
- (12) F. Tian, R.-S.Zhu, J. Zhong, P. Wang, F. Ouyang and G. Cao, *Int. J. Hydrogen Energy*, 2016, **41**, 20156-20171.

(13) J. Dong, Y. Shi, C.-P. Huang, Q. Wu, T. Zeng and W.-F. Yao, *Appl. Catal. B Environ.*, 2019, **243**, 27-35.